IEEE Access
Multidisciplinary ⋮ Rapid Review ⋮ Open Access Journal

Received May 2, 2021, accepted June 8, 2021, date of publication July 2, 2021, date of current version July 13, 2021.

Digital Object Identifier 10.1109/ACCESS.2021.3094358

Frequency Selective Optoelectronic Downconversion of a Terahertz Pulse Using ErAs:In(Al)GaAs Photoconductors

ANUAR DE JESUS FERNANDEZ OLVERA[1], BENEDIKT LEANDER KRAUSE[1], ANDRÉS BETANCUR-PÉREZ[2], UTTAM NANDI[1], CRISTINA DE DIOS[2], PABLO ACEDO[2], (Member, IEEE), AND SASCHA PREU[1], (Member, IEEE)

[1]Department of Electrical Engineering and Information Technology, TU Darmstadt, 64289 Darmstadt, Germany
[2]Department of Electronics Technology, Universidad Carlos III de Madrid, 28911 Leganes, Spain

Corresponding author: Anuar de Jesus Fernandez Olvera (fernandez@imp.tu-darmstadt.de)

This work was supported in part by the European Union Marie Curie Skłodowska Actions through the Innovative Training Network (ITN), (CELTA) under Project 675683, and in part by the European Starting Grant (ERC) (Pho-T-Lyze) under Project 713780.

ABSTRACT We introduce a new scheme for the detection of terahertz pulses based on the frequency selective optoelectronic downconversion of its individual modes with a continous-wave (CW) ErAs:InGaAs photoconductive antenna (PCA) driven by a comb-based CW photonic signal. The detection scheme can be used as metrology tool for the analysis of the fundamental resolution and stability limits of terahertz pulses and the mode-locked-lasers (MLLs) that drives them, as well as an ultra-high-resolution measurement technique for terahertz components or gas spectroscopy. We demonstrate both applications by measuring the linewidth of two frequency components of the particular terahertz pulse analyzed here (one at 75 GHz and one at 340 GHz) and by measuring a very narrowband filter between 70 and 80 GHz. The main advantage of this technique with respect to other terahertz pulse detection schemes is its capability of performing ultra-high-resolution measurements without the need of unpractically long scanning ranges or synchronization of two MLLs.

INDEX TERMS CW photoconductive detectors, ErAs:In(Al)GaAs photoconductors, FreSOD, noise in mode-locked lasers, pulsed terahertz emitters, frequency metrology.

I. INTRODUCTION

Photonic terahertz pulsed systems, also known as terahertz time-domain spectrometers (TDS), have become a powerful tool for non-destructive testing. Their wide bandwidth coverage and real-time capabilities have made them valuable tools for thickness determination of optically-opaque thin layers [1], gas spectroscopy and sensing [2], and quality control of pharmaceuticals [3].

Most modern TDS systems use a single mode-locked laser (MLL) with a repetition rate that ranges between several tens of megahertz and a few hundreds of megahertz in order to generate an optical pulse with a duration of several tens of femtoseconds. This optical pulse is rectified by a photoconductive antenna (PCA) acting as an emitter, producing a pulse with a bandwidth that ranges from DC to several terahertz. The emitted terahertz pulse is then received by a second PCA acting as a receiver, which further receives a delayed version of the original optical pulse. This PCA mixes the two pulses, producing a DC current whose value depends on the relative time delay between them, a process that can actually be seen as a convolution in the time domain. To resolve the temporal structure of the terahertz pulse, a mechanical delay stage scans the time delay between terahertz and optical pulse. The resolution, in time and frequency, depends on the delay interval, and on the number of acquired points during the scan. Due to limited scanning range of the mechanical delay stages, and the associated reduction in dynamic range for extremely long scanning ranges, the resolution in these systems is typically limited to a few gigahertz [4].

Variants of the TDS systems include electronically controlled optical sampling (ECOPS) [5], [6] and asynchronous

The associate editor coordinating the review of this manuscript and approving it for publication was Muguang Wang.

This work is licensed under a Creative Commons Attribution 4.0 License. For more information, see https://creativecommons.org/licenses/by/4.0/

optical sampling (ASOPS) [7]. Both of these schemes use two synchronized MLLs, one of them is sent to the emitting PCA, while the other one, featuring a slightly different repetition rate, is sent to the receiving PCA. The slight difference in repetition rates Δf_{rep} causes a time delay of $(\Delta f_{rep})^{-1}$ between the pulses, a feature that can be exploited to sample the emitted terahertz pulse using the optical pulse sent to the receiver. This removes the need of a mechanical delay stage.

Although the acquisition speed is increased by several orders of magnitude, the implementations of ECOPS or ASOPS achieve frequency resolutions comparable to the ones obtained with traditional pulsed systems. The highest frequency resolution demonstrated with ASOPS is 82.6 MHz, obtained using an acquisition time of 10 seconds [7]. Other implementations have achieved resolutions of around 1 GHz using an acquisition time of 1 second [8]. However, they require the synchronization of two MLLs, which results in complex synchronization electronics and tend to make the system rather expensive.

Less complex implementations using a single-cavity laser emitting two coherent optical pulses with counter-propagating directions [9], or having two different wavelengths [10], have also been demonstrated to be stable enough to reach a resolution around 1 GHz. Still, their operation is not straight-forward.

All of these detection schemes measure the terahertz pulse envelope, not its actual spectral structure. Indeed, the optical pulses generated by the MLLs driving the PCAs have a discrete spectral structure, and so the resulting terahertz pulses. However, the limited spectral resolution of the aforementioned detection schemes normally prevents the identification of such discrete spectral components.

Here, we present a scheme for the optoelectronic detection of terahertz pulses that allows us to see their spectral structure with a resolution way below the common Fourier limited resolution, given by the time window used to acquire the envelope of the detected pulse. We employ two lines of an electro-optically (EO) generated frequency comb to produce a continuous wave (CW) terahertz signal that acts as a photonic local oscillator for the optoelectronic down-conversion of the individual frequency components of a terahertz pulse. We therefore call this scheme Frequency Selective Optoeletronic Downconversion (FreSOD), which is only feasible thanks to the recent developments in telecom-wavelength compatible PCAs [11]–[15]: when acting as emitters in pulsed operation, telecom-wavelength PCAs are now capable of delivering powers in excess of 0.5 mW [16], while CW receivers have shown noise equivalent powers (NEPs) as low as 1.8 fW/Hz [17]. For this particular implementation, we have used state-of-the-art ErAs:In(Al)GaAs PCAs, which have shown an excellent performance in both CW and pulsed operation.

Although purely electronic schemes for the detection of terahertz pulses have already shown their discrete spectral structure [18], their true resolution was still limited by the phase noise inherent to the detection process [19]. Moreover, they were implemented with terahertz electronic sources, making the scheme difficult to tune or to scale in frequency.

The detection scheme presented here is not limited by the phase noise of the detection process, at least not for frequencies above 300 GHz, as we will demonstrate here. This makes it a valuable tool for metrology. In particular, the proposed scheme can be used to measure the phase noise behaviour of the individual components of a terahertz pulse in order to determine its ultimate resolution and stability limits, parameters that are also relevant to study the noise behaviour of the MLLs driving the TDS systems. Since the scheme does not require the use of terahertz electronic sources, it is frequency-scalable and widely tunable. A feature that makes the implementation of high-resolution spectroscopic measurements straight-forward.

As a matter of fact, when a metrologic characterization of the terahertz pulse is not required, the detection scheme can be implemented using simple narrow linewidth CW lasers instead of a comb-based CW system. This would still allow to perform spectroscopic measurements with a much higher resolution than that exhibited by any of the TDS implementations, but at a lower cost.

The article is structured as follows. The theoretical framework describing the spectral structure of terahertz pulses as well as the basic principles of the CW-based detection scheme proposed here are presented in Section II. Section III shows its experimental demonstration by measuring the spectral characteristics of two different spectral components of an analyzed terahertz pulse as well as an application example consisting of a narrow-band filter measurement in the 70-80 GHz range. Finally, future prospects of the technique are discussed in Section IV.

II. THEORETICAL FRAMEWORK

The electric field of the optical pulse generated by a MLL $E_{PL}(t)$ can be described as a sum of N modes

$$E_{PL}(t) = \sum_{n=0}^{N-1} E_{PL,n} e^{i(\omega_{PL}+n\Delta\omega)t+i\theta_n(t)} \tag{1}$$

where n is the mode index, $E_{PL,n}$ and $\theta_n(t)$ the field strength and the timing jitter associated with mode n, respectively, $\omega_{PL} = 2\pi f_{PL}$ the lowest angular frequency contained in the pulse, and $\Delta\omega = 2\pi\Delta f$ the mode spacing [20]. $N\Delta f$ is the bandwidth of the optical pulse, and it is what determines the pulse duration when no chirping is present, as we have assumed here for simplicity.

The optical intensity is given by $I_{PL}(t) = E_{PL}(t)E^*_{PL}(t)$, resulting in

$$I_{PL}(t) = I_{PL,0} + \sum_{n=1}^{N-1} I_{PL,n}\cos(\Delta\omega_n ft + \phi_n(t)) \tag{2}$$

where $I_{PL,0}$ is the average intensity, $I_{PL,n}$ the intensity of mode n, $\Delta\omega_n = n\Delta\omega$, and $\phi_n(t)$ the timing jitter associated with the degree of coherence between optical modes with a separation of n.

The photoconductive material in the PCA absorbs the energy in the optical pulse at a rate given by $I_{PL}(t)$, resulting in the excitation of an electron-hole pair carrier density $n_{pl}(t)$ that follows the optical pulse intensity envelope [21], i.e.

$$n_{pl}(t) \sim I_{PL}(t). \tag{3}$$

As indicated by Eq. 2 and 3, the frequencies of the modes generated in the PCA are the result of the frequency differences that exist between the modes of the optical pulse. Consequently, $n_{pl}(t)$ does not possess a carrier envelope offset. However, like in an optical frequency comb, each of the modes in $n_{pl}(t)$ does possess a very narrow linewidth. This is because all the modes are phase-locked given that they all share the same origin: the MLL driving the PCA. In fact, the linewidth of the modes in $n_{pl}(t)$ is an indication of the degree of phase-locking, or coherence, between optical modes sharing the same frequency difference. Therefore, its characterization is a useful tool for the analysis of the phase noise behaviour in MLLs.

Applying a DC bias U_{DC} to the PCA transforms $n_{pl}(t)$ into a net drift current density $j_{pl}(t)$, whose magnitude is given by

$$j_{pl}(t) \sim n_{pl}(t) e v_{pl} \tag{4}$$

where e is the electron charge, and v_{pl} the drift velocity, with an approximate value of

$$v_{pl} = \mu_{AC} \frac{U_{DC}}{d_{eff}} \tag{5}$$

μ_{AC} being the AC charge mobility of the respective carrier type, and d_{eff} the length of the field line that accelerates the charge. In the following, we neglect the actual carrier dynamics of the photoconductive material in the PCA [22]. We continue with average values for the velocities and we also neglect hole contributions as these are very small due to their large effective mass as compared to that of the electrons. Thus, we can assume that the electric field amplitude of the pulse emitted by the PCA $e_{pl}(t)$ is proportional to the current density fed to the antenna [22], hence

$$e_{pl}(t) \sim \sum_{n=1}^{N-1} e_{pl,n} \cos\left(\Delta\omega_n t + \phi_n(t)\right) \tag{6}$$

where $e_{pl,n} \sim j_{pl,n}$. The proportionality constant is related to the radiation resistance of the antenna and may include frequency-dependent lifetime and RC roll-offs. As opposed to the usual understanding of a terahertz pulse as an ultra-broadband signal without any spectral substructure, Eq. 6 shows that the pulse is in fact composed of discrete modes with a mode spacing given by the repetition rate $\Delta\omega$, a representation that can also be seen as its Fourier series. Indeed, what we have is an unstabilized terahertz frequency comb if the MLL is just passively locked.

The CW receiver consists of a PCA whose photoconductive material absorbs the energy of two CW laser signals with a frequency offset f_{lo}. As in the previous case, the excitation of electron-hole pairs by the laser signals results in a carrier density n_{cw} that follows the optical intensity envelope, which for the two CW laser signals of this case results in

$$n_{cw}(t) = n_0 + n_{ac} \cos\left(\omega_{lo} t + \phi_{lo}(t)\right) \tag{7}$$

where n_0 is the excited DC carrier density, n_{ac} the coefficient of its AC counterpart, $\omega_{lo} = 2\pi f_{lo}$ and $\phi_{lo}(t)$ the timing jitter associated with the degree of coherence between the two CW optical modes.

Like in the pulsed case, an applied bias generates a current density out of the optically generated carrier density. Here, however, the bias originates from the terahertz field $e_{pl}(t)$ received by the antenna incorporated in the CW PCA. This causes a modulation of the drift velocity $v_{cw}(t) \sim e_{pl}(t)$, which in turn produces a drift current density $j_{cw}(t)$ with magnitude

$$j_{cw}(t) \sim n_{cw}(t) e_{pl}(t). \tag{8}$$

Thus, $j_{cw}(t)$ will be composed of three sets of terms

$$\begin{aligned} j_{cw}(t) \sim & \sum_{n=1}^{N-1} e_{pl,n} \cos\left(\Delta\omega_n t + \phi_n(t)\right) \\ & + \sum_{n=1}^{N-1} e_{pl,n} \cos\left((\Delta\omega_n - \omega_{lo})t + \phi_n(t) - \phi_{lo}(t)\right) \\ & + \sum_{n=1}^{N-1} e_{pl,n} \cos\left((\Delta\omega_n + \omega_{lo})t + \phi_n(t) + \phi_{lo}(t)\right). \end{aligned} \tag{9}$$

where, again, the proportionality constants are related to the radiation resistance of the receiving antenna and to the RC and lifetime roll-offs. Almost all terms in Eq. 9 lie outside the detection bandwidth $\Delta\omega_{det}$, which typically ranges from DC to a few MHz at best, depending on the post-detection electronics connected to the CW PCA. Only the terms with a frequency that is low enough to be within $\Delta\omega_{det}$ can be amplified by the post-detection electronics, i.e. only the terms that result from the frequency differences can be detected. This occurs if

$$\Delta\omega_{det} > |\omega_{lo} - \Delta\omega_n|. \tag{10}$$

Therefore, appropriate choice of ω_{lo} allows only one mode of the terahertz pulse to be detected, resulting in a detected current $i_{det}(t)$ given by

$$i_{det}(t) \sim e_{pl,n} \cos\left((\Delta\omega_n - \omega_{lo})t + \phi_{det}(t)\right) \tag{11}$$

where $\phi_{det}(t) = \phi_n(t) - \phi_{lo}(t)$ is the total timing jitter in the detected signal. Although the timing jitter is a stochastic variable that fully characterizes the phase noise of a CW signal, its long-term mean and its long-term variance do not converge. Therefore, we will use its short-term versions, in particular, its short-term variance σ_s^2 and short-term standard deviation σ_s, for our analysis.[1]

[1]The short term variance is also known as cycle-to-cycle jitter, and it only measures the variance of each period with respect to the average of a short period of time. It does not consider long-term drifts. It is also possible to analyze the long-term variations of the phase, but one needs to use the Allan deviation instead.

For the case $\sigma_s(\phi_{lo}) \ll \sigma_s(\phi_n)$, $\sigma_s(\phi_{det})$ is a good measure of the timing jitter, or phase noise, in the selected mode of the terahertz pulse. Otherwise, the standard deviation of the detected phase is given by

$$\sigma_s(\phi_{det}) = \sqrt{\sigma_s^2(\phi_{lo}) + \sigma_s^2(\phi_n)}, \tag{12}$$

but even for the latter case, the average peak value of $i_{det}(t)$ will still be proportional to the average peak value of $e_{pl,n}$, meaning that one can still perform measurements with the resolution of each of the modes in the emitted pulse, as demonstrated in [18], just without the capability of characterizing the behaviour of $\sigma_s(\phi_n)$.

Fig. 1 shows a graphical representation of the frequency selection process in FreSOD. The main difference between classical TDS systems and this detection technique is the ability to resolve the individual modes of the terahertz pulse regardless of the time window Δt used. In classical TDS systems, Δt limits the frequency resolution according to the Heisenberg uncertainty principle $\Delta t \Delta f \geq 1/2$, making almost impossible to achieve the resolution required to resolve each individual mode.

As a detection technique, the main advantages of FreSOD can be summarized as follows:

1) It allows a Hz-level characterization of the phase noise of each of the individual modes in the terahertz pulse when the phase noise in the CW signal is smaller than that of the individual modes. Such is the case for a comb-based CW system, at least for higher frequencies.
2) It allows to perform spectroscopy with a stepwise resolution equal to the frequency spacing of the modes in the terahertz pulse, i.e. the repetition rate of the MLL. With typical values around 100 MHz, FreSOD resolution is already 1.5 orders of magnitude better than the resolution of typical TDS systems, with resolutions in the order of a few GHz.
3) When a precise phase noise characterization of the terahertz pulse is not required, a simpler version of the system using two simple CW lasers instead of a comb is also possible. Such setups are less demanding and less expensive than the fully electronic one shown in [18] and also than ASOPS or ECOPS. In general, standard CW laser systems offer tuning ranges between 1 THz and several THz [23], however, their increased phase noise would require the implementation of faster post-detection electronics able to follow the detected signal jitter. This might increase the overall noise level, and hence might reduce the available signal-to-noise ratio.

III. EXPERIMENTAL DEMONSTRATION

In the next subsections we show the experimental demonstration of the two possible applications of FreSOD: the precise phase noise characterization of terahertz pulses, and the realization of extremely high-resolution (sub-)terahertz measurements using terahertz pulses. In subsection A we describe the two different setups used to demonstrate each of these applications. In subsection B we show the results of the first of such applications: a comparison between the phase noise behaviour of the 750th mode and the 3400th mode of the particular terahertz pulsed analyzed. In subsection C we show the results of the second one: a high-resolution measurement of a narrow-band filter between 70 and 80 GHz.

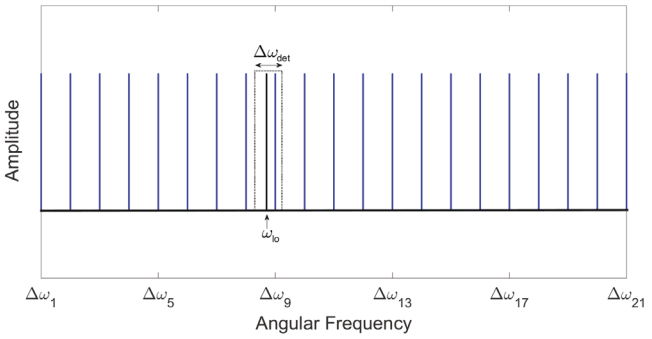

FIGURE 1. Graphical representation of the mode selection process in the angular frequency domain. The dashed rectangle represents the detection bandwidth.

A. DESCRIPTION OF THE EXPERIMENTAL SETUPS

We used an ErAs:In(Al)GaAs pulsed PCA driven by a passively locked MLL from Menlo Systems as a pulsed emitter. The ErAs:In(Al)GaAs pulsed PCA, similar to the one described in [14], emitted an average terahertz power of 76 μW when biased with a voltage of 200 V. The MLL had an optical output power of 42 mW, a nominal mode spacing of 100 MHz, a duration of less than 90 fs (as measured by an interferometric autocorrelator) and a center wavelength of 1560 nm. This corresponds to a bandwidth of at least 8.32 THz [20]. However, several terahertz measurements suggest a maximum bandwidth of 6.5 THz due to losses at the upper spectral end caused by the roll-offs of the PCAs as well as by the absorption tails of the Reststrahlenband of the InP substrate of the photoconductor. Therefore, we had $\Delta f = 100$ MHz, $N\Delta f = 6.5$ THz, and $N = 65000$.

For detection, we have used a CW ErAs:InGaAs PCA similiar to the one described in [17], driven by two selected modes of an EO generated optical frequency comb. This photonic local oscillator had an extremely low phase-noise and thus enabled us to use post-detection electronics with a low noise level.

A different comb-based CW system was implemented for each of the demonstrated applications. For the comparison of the phase noise behaviour between the two terahertz modes, we employed a comb-based CW system using optical injection locking for the mode selection [24]. In this technique, a discrete-mode laser acts as an active filter by making the resonant frequency of its cavity match the frequency of the mode to be selected. This is done by manually adjusting the laser current and temperature, while monitoring the laser output spectrum. Locking is achieved when the laser output mode

does not change its frequency anymore, even after the laser temperature or its current are changed. The complete CW system is depicted Fig. 2 (a). It consists of a discrete-mode master laser whose output is modulated by two cascaded EO phase modulators (EOMs). The phase modulation results in the generation of sidebands, as mathematically described by the Jacobi-Anger expansion [25]. The sidebands compose an optical frequency comb in which all the modes share almost the same timing jitter, mostly coming from the common laser source. The optical frequency comb is then split into two branches. In each of the two branches, a discrete-mode laser selects the desired mode via optical injection locking. The narrow linewidth exhibited by such lasers makes the injection-locking filtering highly selective, allowing a very high mode suppression ratio with excellent tuning capabilities. The selected modes in each of the branches with mode index difference m, are then combined and subsequently amplified by an EDFA to reach 30 mW. These two selected modes generate the CW local oscillator in the ErAs:InGaAs PCA via the frequency-difference generation mechanism, resulting in a local oscillator with frequency $f_{lo} = mf_{RF}$, where f_{RF} can be chosen between 5 and 20 GHz. Afterwards, the ErAs:InGaAs PCA was connected to a TIA with a gain of 3.3×10^6V/A and a bandwidth of 120 kHz, and from there to a lock-in amplifier with spectral analysis capabilities.

The gain of the injection-locked lasers drastically reduces the phase noise introduced by the EDFA in this setup, which only required a gain of 3 dB. This guarantees a superior optical signal-to-noise ratio for higher local oscillator frequencies, a condition that is necessary to perform an adequate spectral analysis, especially in terms of phase noise. In addition to that, the frequency-difference generation mechanism of the CW PCA removes all the timing jitter from the master laser that is common to all the EO generated modes [26], ensuring the spectral purity of photonic local oscillator. The frequency-difference mechanism also ensures its spectral accuracy, given that its frequency only depends on the frequency difference between the optical modes, which is entirely set by the RF generator. The 3-dB linewidth of the RF generator used in this system was measured to be narrower than 1 Hz with a frequency stability better than 0.33 Hz/s. Its frequency accuracy is as good as its last calibration, but absolute frequency accuracy can be achieved by locking the RF generator to a frequency standard, as demonstrated in [24]. This would also improve the frequency stability.

For the high-resolution measurement of the narrow-band filter, we used a comb-based CW system employing a digitally tunable narrow-bandwidth optical filter for mode selection. The digitally tunable optical filter allowed us to perform a frequency sweep without the need to manually tune the lasers every time the frequency is changed, although with an increased phase noise due to the high amplification required before and after filtering. The complete CW system is depicted in Fig. 2 (b). It consists of a single DFB laser whose output is amplified up to 280 mW by an EDFA, and then split into two branches. The optical signal in the first

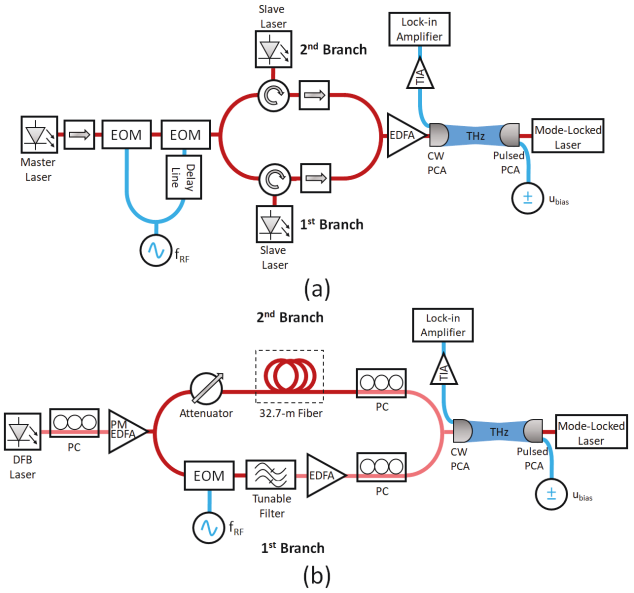

FIGURE 2. (a) Schematic diagram of the comb-based CW optical system utilized for the comparison between the phase noise behaviour of the 750th and 3400th modes. (b) Schematic diagram of the comb-based CW optical system utilized for the measurement of the narrowband bandpass filter. The pale red fiber represents non-PM fiber, while the bright red represents PM fiber. The polarization between the different fibers was matched using polarization controllers (PCs).

branch is phase-modulated by an EOM driven by a RF generator with frequency f_{RF}. One of the modes is then selected by the digitally tunable optical filter, and subsequently amplified by a second EDFA. Next, the selected mode m is combined with the main optical mode of the DFB laser carried by the second branch, where 32.7 m of optical fiber were added to equalize the optical lengths in both branches. The optical signal containing the combined modes, with an optical power of 15 mW, is used to generate CW local oscillator in the ErAs:InGaAs PCA with a frequency $f_{lo} = mf_{RF}$. As in the previous setup, a TIA with a gain of 3.3×10^6 V/A and a bandwidth of 120 kHz, as well as a lock-in amplifier were used as post detection electronics.

It might be tempting to think that the interferometric structure of the systems shown in Fig. 2 might have generated additional power fluctuations. However, the optical signal travelling in each of the branches had a different frequency, making interference-based fluctuations not a significant problem.

B. APPLICATION 1: COMPARISON OF THE PHASE NOISE BETWEEN THE 750th AND THE 3400th TERAHERTZ MODES

In the previous section, the phase noise of a given terahertz mode and that of the CW local oscillator were represented in time domain by the timing jitter, given by $\phi_n(t)$ and $\phi_{cw}(t)$, respectively. In particular, we centered our attention on their short-term statistics, and the condition established for the short-term statistics of $\phi_{det}(t)$ to be a good indicator of the short-term statistics of $\phi_n(t)$ was that $\sigma_s(\phi_{cw}) \ll \sigma_s(\phi_n)$.

In practice, the short-term timing jitter statistics are somewhat difficult to measure in the time domain, so we will use the corresponding linewidth in the frequency domain instead, as it can be easily measured using a spectrum analyzer.

The relationship between short-term timing jitter statistics, phase noise and linewidth has been studied extensively. Here, we will adopt the simplified relationship proposed in [27], in which the phase noise, or more precisely, the phase noise spectral density, $\mathcal{L}(f)$ is expressed as

$$\mathcal{L}(f) = \frac{1}{\pi} \frac{\delta f}{(\delta f)^2 + f^2} \tag{13}$$

where $2\delta f$ is the full width half maximum (FWHM) linewidth of the signal and f is the offset from the center frequency. We have implicitly assumed a Lorentzian line shape for simplicity here, however, a corresponding expression can also be obtained for a Gaussian line shape.

In an equivalent manner, the phase noise can also be written as a function of the short-term timing jitter variance $\sigma_s^2(\phi)$, resulting in

$$\mathcal{L}(f) = \frac{\sigma_s^2(\phi_{det}) f_c^3}{f^2} \tag{14}$$

where f_c is the center frequency of the signal. Equating Eq. 13 and Eq. 14, and measuring the phase noise in a time scale in which $f \gg \delta f$ allows one to write the FWHM linewidth as

$$\delta f \approx \pi f_c^3 \sigma_s^2(\phi_{det}). \tag{15}$$

Therefore, for a given frequency, a small linewidth is directly proportional to a small short-term timing jitter variance. This means that the requirement of having a local oscillator with a much smaller timing jitter variance or standard deviation than that of the mode to be analyzed can be directly translated as having a local oscillator linewidth much narrower than that of the mode to be analyzed.

Here, we analyzed the linewidth of two emitted terahertz modes whose frequency was far enough apart to exhibit a significant difference: the 750^{th} and the 3400^{th} mode. For each of the modes, we recorded the downconverted power spectrum obtained using the CW setup of Fig. 2 (a). A sample spectrum of the optical signal used to generate the CW local oscillator for the downconversion of the 3400^{th} mode is shown in Fig. 3, highlighting the high frequency capabilities of the injection-locked-based CW system.

Fig. 4 shows the downconverted spectrum of the 750^{th} mode. For this measurement $\Delta f = 99.888834$ MHz, as measured by a fast photodiode connected to a spectrum analyzer. This indicated that its actual frequency was 74.9166255 GHz. Hence, we set f_{RF} to 7.49166025 GHz, and m to 10. This resulted in a local oscillator frequency of 74.9166025 GHz and an intermediate frequency of around 23 kHz. Correspondingly, the center frequency of the spectrum analyzer integrated in the lock-in amplifier was set to 23.25 kHz, the resolution bandwidth to 0.817 Hz, and the sweep time to 1.22 s. A FWHM linewidth of 1.8 Hz was found to fit

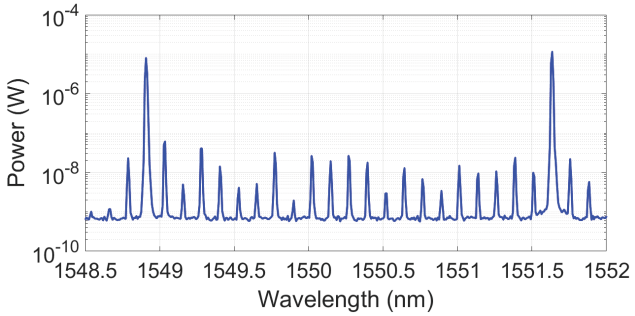

FIGURE 3. Optical spectrum of the selected modes for the CW local oscillator generation used to downconvert the 3400^{th} mode obtained using the experimental setup of Fig. 2(a).

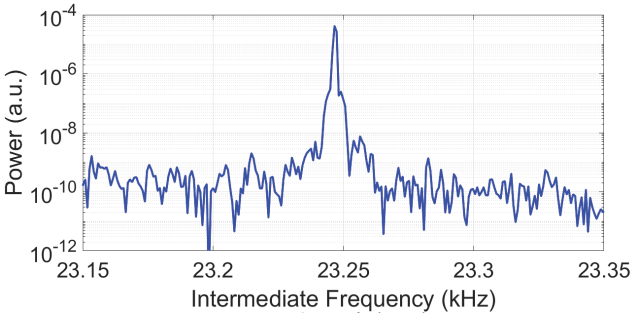

FIGURE 4. Downconverted power spectrum of the 750^{th} mode located at 74.9166255 GHz. Resolution bandwidth: 0.817 Hz. Sweep time: 1.22 s. FWHM linewidth: 1.8 Hz.

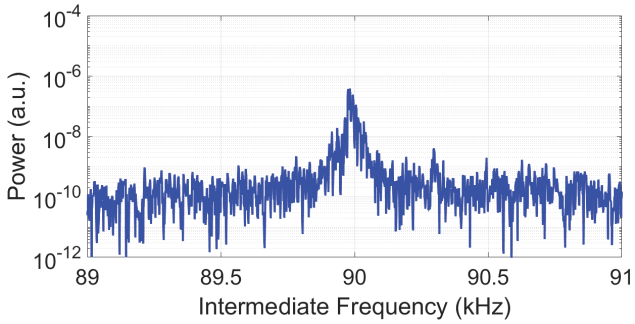

FIGURE 5. Downconverted power spectrum of the 3400^{th} mode located at 339.6209272 GHz. Resolution bandwidth: 1.63 Hz. Sweep time: 0.61 s. FWHM linewidth: 20 Hz.

the spectrum. Given that the measured spectrum is the convolution between the local oscillator spectrum and the 750^{th} mode spectrum, as expressed in the time-domain by Eq. 12, and that the local oscillator linewidth is also on the Hz level, the value of 1.8 Hz can only be considered as an upper limit for the linewidth of that mode. An RF generator with a better phase noise performance would have been needed to perform a more accurate characterization.

Fig. 5 shows the downconverted spectrum for the 3400^{th} mode. In this case, $\Delta f = 99.888508$ MHz, i.e. 326 Hz lower than for the previous measurement due to the random drifts in the passively-locked MLL long-term phase

noise. Therefore, the terahertz frequency of this mode was rather 339.6209272 GHz. In order to detect it, we set $f_{RF} = 15.4373108987$ GHz and $m = 22$ to get a local oscillator frequency of 339.6208397714 GHz, with a corresponding intermediate frequency of around 90 kHz. The spectrum analyzer was tuned accordingly, with the resolution bandwidth set to 1.63 Hz, and the sweep time to 0.611 s. A FWHM linewidth of 20 Hz was found to fit the spectrum. The broadening in the linewidth can be clearly attributed to the increased phase noise of the 3400^{th} mode, not to the CW local oscillator anymore. This is because the previous measurement already gave us an upper limit on the local oscillator linewdith. Even if we would assume a worst-case scenario in which the linewidth of the local oscillator increases as a square of mode number difference [26], the increase in the mode number difference would not explain a factor of 11 broader linewidth (Although for this kind of photonic local oscillator, we would indeed expect an almost constant linewidth as the mode number difference increases).

Still, the phase noise performance of the passively-locked MLL is quite impressive: a linewidth of about 20 Hz for a tone generated by photomixing modes that are 3400 modes apart. This is somewhat expected, the linewidth of microwave signals generated by photomixing different modes of passively-locked MLLs has been shown to be much narrower than those generated using actively locked MLLs, at least for the very first modes [28]. However, there is still a lack of theoretical understanding on how the phase noise behaves in passively locked MLLs [29], [30], mainly due to the lack of experimental data for its behavior at higher order modes. Therefore, we believe that FreSOD might help to fill this gap.

C. APPLICATION 2: CHARACTERIZATION OF A NARROWBAND FILTER IN THE 70–80 GHz RANGE

For the measurement of the filter, we swept the photonic CW local oscillator of Fig. 2 (b) between 68.823158 GHz and 79.91076484 GHz in steps equal to Δf. Such frequencies were determined by the actual value of Δf, measured to be 99.88835 MHz for this case. The measurement range was limited to 79.91076484 GHz due to the reduced frequency capabilities of the photonic CW local oscillator of Fig. 2 (b). A sample spectrum of the optical signal generated using this photonic CW system is shown in Fig. 6.

For the sweep, m was set to 4, and f_{RF} was varied between 17.2057895 GHz and 19.9776912125 GHz in 24.9720875 MHz steps. This resulted in an intermediate frequency centered around 85 kHz for each of the downconverted modes. Therefore, the local oscillator of the lock-in amplifier was tuned to 85.6 kHz, the sampling frequency was set to 26.79 kHz, and the detection bandwidth was set to 4 kHz (corresponding to an integration time of 11.97 μs). We remark that given that the MLL was not actively stabilized, no external reference could be given to the lock-in amplifier for the demodulation of each of the detected modes. However, since the random drifts in the long-term frequency

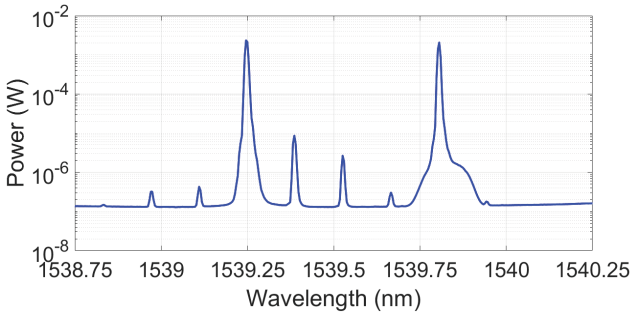

FIGURE 6. Optical spectrum of the selected modes for the CW local oscillator generation for $f_{RF} = 17.2057895$ GHz and $m = 4$ obtained using experimental setup of Fig. 2(b).

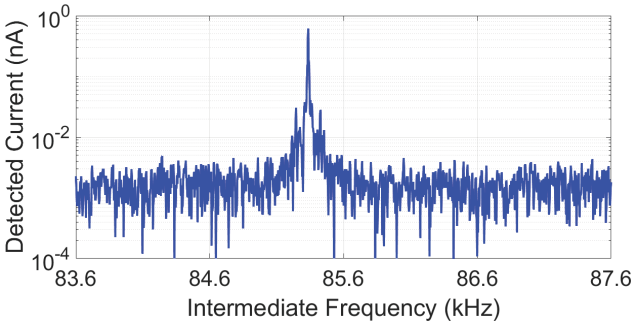

FIGURE 7. Downconverted current spectrum obtained when f_{lo} was tuned to detect the 750^{th} mode located at $\Delta f_{750} = 74.916243$ GHz.

stability of the MLL were much smaller than the measurement time, such drifts did not represent a major problem for the measurement.

Fig. 7 shows a sample downconverted spectrum for $\Delta f_{750} = 74.9162625$ GHz before demodulation with the lock-in amplifier. The two side lobes appearing in the spectrum originate from the DFB laser used to generate the CW local oscillator. Fig. 8 shows the peak detected current obtained with (black) and without (blue; reference measurement) the filter on the free-space terahertz path for the swept frequency range. Each value was obtained after averaging 50 individual measurements at each frequency point in order to increase the measurement precision. The total acquisition of the 224 frequency points, each one averaged 50 times, took around 4 mins, i.e. 2 mins (112 points) per sweep.

Fig. 9 shows the power transmission coefficient calculated with the values shown in Fig. 8 after applying an 11^{th} order moving average filter. The figure also shows the power transmission coefficient obtained with a commercial TDS system featuring a frequency resolution of 2.49 GHz. The moving average filter applied to the data obtained with FreSOD was required to average out the effect of unwanted reflections within the setup, which appear as interference fringes superimposed on the actual transmission coefficient [31]. This fact underscores the extremely high-frequency resolution achieved, ultimately leading to a more accurate characterization of the filter. In a normal TDS system, undesired

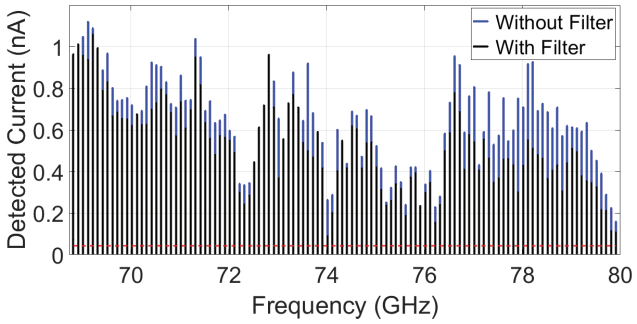

FIGURE 8. Comparison between the peak detected currents with (black) and without (blue) filter on the terahertz path. The dashed red line represents the detection limit for this measurement.

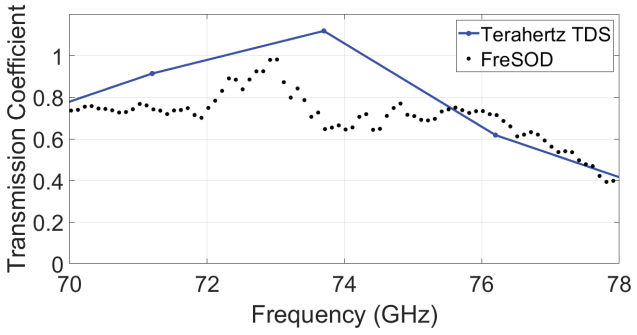

FIGURE 9. Comparison between the power transmission coefficient obtained with FreSOD (black dots) and the one obtained with a commercial TDS system (blue line). One point of the TDS measurement is larger than one due to the imperfections of the TDS technique at such low frequencies as discussed in the text.

reflections appear as echoes in the time domain, i.e. as copies of the main pulse that repeat themselves in time and that can be time-gated. In FreSOD, those undesired reflections appear as superimposed oscillations directly in the frequency domain. Since the scanning range for our TDS measurement was limited to 400 ps, part of the information for some of the frequency components is missing, resulting in a decreased accuracy, causing the transmission coefficient obtained with the commercial TDS system to be higher than one at 73.7 GHz. Additionally, we must also consider that TDS systems might turn inaccurate below $\sim$ 150 GHz, particularly, because the waves at those frequencies exhibit very long periods, and the windowing required to obtained the spectrum might modify the results for such low frequencies.

All in all, the comparison between the TDS and the FreSOD measurement clearly shows the advantages of the superior resolution, which is far beyond the classical Fourier-transform (or Heisenberg)-limited resolution of traditional TDS systems.

IV. CONCLUSION

We have experimentally demonstrated the frequency selective optoelectronic downconversion of the individual modes composing a terahertz pulse using ErAs:In(Al)GaAs PCAs. In particular, we have used an ErAs:In(Al)GaAs pulsed PCA driven by a passively-locked MLL as a terahertz pulsed emitter, and a ErAs:InGaAs PCA driven by a comb-based CW system as a downconverter. With this configuration, we have shown a stepwise frequency resolution smaller than 100 MHz, which is about 1 order of magnitude better than the resolution achieved with the same emitter in a TDS system. Additionally, we have shown that the emitted modes using this particular pulsed system can have a linewidth as narrow as 20 Hz for frequencies as high as 340 GHz.

The frequency coverage of our comb-based CW implementation is limited by the maximum achievable frequency of the CW system and by the available terahertz power in each of the modes of the terahertz pulse. Both factors can be significantly improved. Similar EO generated frequency combs with a frequency coverage of around 1 THz have already been demonstrated [32], while pulsed PCAs emitting terahertz powers almost one order of magnitude higher than the one used here have also been shown [16]. This would allow a thorough characterization of the phase noise evolution of the several thousands of modes composing the terahertz pulses generated by passively locked MLLs. Such characterization could help in the development of accurate noise models for passively-locked MLLs, not only for terahertz pulses. Even though we have only analyzed the short-term phase noise characteristics in this article, it is also possible to analyze the long-term characteristics with the same technique by locking the comb-based CW terahertz system to a frequency standard [24].

Thus, the combination of passively stabilized terahertz combs, i.e. terahertz pulses, and CW terahertz systems enables a new class of spectroscopic systems with stepwise frequency resolutions as small as the repetition rate of the terahertz comb. This, without the need of unpractically long scanning ranges, mechanical delay stages or dual frequency comb systems. Indeed, significantly simpler versions of FreSOD can be constructed by replacing the comb-based CW system by two independent narrow-linewidth CW lasers as long as the detection bandwidth is significantly higher than the CW-terahertz signal linewidth. This is easily achievable with external cavity lasers, exhibiting linewidths as low as 5 kHz [26].

REFERENCES

[1] T. Pfeiffer, S. Weber, J. Klier, S. Bachtler, and D. Molter, "Terahertz thickness determination with interferometric vibration correction for industrial applications," *Opt. Exp.*, vol. 26, no. 10, pp. 12558–12568, 2018.

[2] R. M. Smith and M. A. Arnold, "Selectivity of terahertz gas-phase spectroscopy," *Anal. Chem.*, vol. 87, no. 21, pp. 10679–10683, Nov. 2015.

[3] J. A. Zeitler, P. F. Taday, D. A. Newnham, M. Pepper, K. C. Gordon, and T. Rades, "Terahertz pulsed spectroscopy and imaging in the pharmaceutical setting–a review," *J. Pharmacy Pharmacol.*, vol. 59, no. 2, pp. 209–223, Feb. 2010.

[4] J. Xu, T. Yuan, S. Mickan, and X.-C. Zhang, "Limit of spectral resolution in terahertz time-domain spectroscopy," *Chin. Phys. Lett.*, vol. 20, no. 8, pp. 1266–1268, Aug. 2003.

[5] M. Yahyapour, A. Jahn, K. Dutzi, T. Puppe, P. Leisching, B. Schmauss, N. Vieweg, and A. Deninger, "Fastest thickness measurements with a terahertz time-domain system based on electronically controlled optical sampling," *Appl. Sci.*, vol. 9, no. 7, p. 1283, Mar. 2019.

[6] Y. Kim and D.-S. Yee, "High-speed terahertz time-domain spectroscopy based on electronically controlled optical sampling," *Opt. Lett.*, vol. 35, no. 22, pp. 3715–3717, 2010.
[7] T. Yasui, E. Saneyoshi, and T. Araki, "Asynchronous optical sampling terahertz time-domain spectroscopy for ultrahigh spectral resolution and rapid data acquisition," *Appl. Phys. Lett.*, vol. 87, no. 6, Aug. 2005, Art. no. 061101.
[8] Y.-D. Hsieh, S. Nakamura, D. G. Abdelsalam, T. Minamikawa, Y. Mizutani, H. Yamamoto, T. Iwata, F. Hindle, and T. Yasui, "Dynamic terahertz spectroscopy of gas molecules mixed with unwanted aerosol under atmospheric pressure using fibre-based asynchronous-optical-sampling terahertz time-domain spectroscopy," *Sci. Rep.*, vol. 6, no. 1, Sep. 2016, Art. no. 28114.
[9] R. D. Baker, N. T. Yardimci, Y.-H. Ou, K. Kieu, and M. Jarrahi, "Self-triggered asynchronous optical sampling terahertz spectroscopy using a bidirectional mode-locked fiber laser," *Sci. Rep.*, vol. 8, no. 1, Dec. 2018, Art. no. 14802.
[10] G. Hu, T. Mizuguchi, R. Oe, K. Nitta, X. Zhao, T. Minamikawa, T. Li, Z. Zheng, and T. Yasui, "Dual terahertz comb spectroscopy with a single free-running fibre laser," *Sci. Rep.*, vol. 8, no. 1, Dec. 2018, Art. no. 11155.
[11] R. B. Kohlhaas, S. Breuer, S. Nellen, L. Liebermeister, M. Schell, M. P. Semtsiv, W. T. Masselink, and B. Globisch, "Photoconductive terahertz detectors with 105 dB peak dynamic range made of rhodium doped InGaAs," *Appl. Phys. Lett.*, vol. 114, no. 22, Jun. 2019, Art. no. 221103.
[12] N. T. Yardimci, H. Lu, and M. Jarrahi, "High power telecommunication-compatible photoconductive terahertz emitters based on plasmonic nano-antenna arrays," *Appl. Phys. Lett.*, vol. 109, no. 19, 2016, Art. no. 191103.
[13] U. Nandi, J. C. Norman, A. C. Gossard, H. Lu, and S. Preu, "1550-Nm driven ErAs: In (Al) GaAs photoconductor-based terahertz time domain system with 6.5 THz bandwidth," *J. Infr., Millim., THz Waves*, vol. 39, no. 4, pp. 340–348, Apr. 2018.
[14] U. Nandi, K. Dutzi, A. Deninger, H. Lu, and J. Norman, "ErAs: In (Al) GaAs photoconductor-based time domain system with 4.5 THz single shot bandwidth and emitted terahertz power of 164 μW," *Opt. Lett.*, vol. 45, no. 10, pp. 2812–2815, 2020.
[15] A. D. J. F. Olvera, H. Lu, A. C. Gossard, and S. Preu, "Continuous-wave 1550 nm operated terahertz system using ErAs: In (Al) GaAs photoconductors with 52 dB dynamic range at 1 THz," *Opt. Exp.*, vol. 25, no. 23, pp. 29492–29500, 2017.
[16] R. B. Kohlhaas, S. Breuer, L. Liebermeister, S. Nellen, M. Deumer, M. Schell, M. P. Semtsiv, W. T. Masselink, and B. Globisch, "637 μW emitted terahertz power from photoconductive antennas based on rhodium doped InGaAs," *Appl. Phys. Lett.*, vol. 117, no. 13, Sep. 2020, Art. no. 131105.
[17] A. Fernandez Olvera, A. Roggenbuck, K. Dutzi, N. Vieweg, H. Lu, A. Gossard, and S. Preu, "International system of units (SI) traceable noise-equivalent power and responsivity characterization of continuous wave ErAs:InGaAs photoconductive terahertz detectors," *Photonics*, vol. 6, no. 1, p. 15, Feb. 2019.
[18] D. G. Pavelyev, A. S. Skryl, and M. I. Bakunov, "High-resolution broadband terahertz spectroscopy via electronic heterodyne detection of a photonically generated terahertz frequency comb," *Opt. Lett.*, vol. 39, no. 19, pp. 5669–5672, 2014.
[19] A. Hati, C. Nelson, and D. Howe, "PM noise measurement at W-band," *IEEE Trans. Ultrason., Ferroelectr., Freq. Control*, vol. 61, no. 12, pp. 1961–1966, Dec. 2014.
[20] M. Wollenhaupt, A. Assion, and T. Baumert, "Femtosecond laser pulses: Linear properties, manipulation, generation and measurement," in *Handbook Lasers Optics*, A. Träger, Ed. New York, NY, USA: Springer, 2007, pp. 937–983.
[21] S. Preu, G. H. Döhler, S. Malzer, L. J. Wang, and A. C. Gossard, "Tunable, continuous-wave terahertz photomixer sources and applications," *J. Appl. Phys.*, vol. 109, no. 6, Mar. 2011, Art. no. 061301.
[22] S. Preu, "A unified derivation of the terahertz spectra generated by photoconductors and diodes," *J. Infr., Millim., THz Waves*, vol. 35, no. 12, pp. 998–1010, Dec. 2014.
[23] A. J. Deninger, A. Roggenbuck, S. Schindler, and S. Preu, "2.75 THz tuning with a triple-DFB laser system at 1550 nm and InGaAs photomixers," *J. Infr., Millim., THz Waves*, vol. 36, no. 3, pp. 269–277, Mar. 2015.
[24] A. R. Criado, C. de Dios, E. Prior, G. H. Dohler, S. Preu, S. Malzer, H. Lu, A. C. Gossard, and P. Acedo, "Continuous-wave sub-THz photonic generation with ultra-narrow linewidth, ultra-high resolution, full frequency range coverage and high long-term frequency stability," *IEEE Trans. THz Sci. Technol.*, vol. 3, no. 4, pp. 461–471, Jul. 2013.
[25] MathWorld-A Wolfram Web Resource. *Jacobi-Anger Expansion*. Accessed: Mar. 21, 2021. [Online]. Available: https://mathworld.wolfram.com/Jacobi-AngerExpansion.html
[26] Z. Tong, A. O. Wiberg, E. Myslivets, B. P. Kuo, N. Alic, and S. Radic, "Spectral linewidth preservation in parametric frequency combs seeded by dual pumps," *Opt. Exp.*, vol. 20, no. 16, pp. 1710–1719, 2012.
[27] Keysight Technologies. (2017). *Overview on Phase Noise and Jitter*. [Online]. Available: https://www.keysight.com/de/de/assets/7018-01984/technical-overviews/5990-3108.pdf
[28] D. von der Linde, "Characterization of the noise in continuously operating mode-locked lasers," *Appl. Phys. B, Lasers Opt.*, vol. 39, no. 4, pp. 201–217, Apr. 1986.
[29] H. A. Haus and A. Mecozzi, "Noise of mode-locked lasers," *IEEE J. Quantum Electron.*, vol. 29, no. 3, pp. 983–996, Mar. 1993.
[30] R. Paschotta, "Timing jitter and phase noise of mode-locked fiber lasers," *Opt. Exp.*, vol. 18, no. 5, pp. 5041–5054, 2010.
[31] A. Roggenbuck, K. Thirunavukkuarasu, H. Schmitz, J. Marx, A. Deninger, I. C. Mayorga, R. Güsten, J. Hemberger, and M. Grüninger, "Using a fiber stretcher as a fast phase modulator in a continuous wave terahertz spectrometer," *J. Opt. Soc. Amer. B, Opt. Phys.*, vol. 29, no. 4, pp. 614–620, 2012.
[32] E. Prior, C. de Dios, R. Criado, M. Ortsiefer, P. Meissner, and P. Acedo, "1 THz span optical frequency comb using VCSELs and off the shelf expansion techniques," in *Proc. Conf. Lasers Electro-Opt.*, 2016, San Jose, CA, USA, 2016, Paper. SF2O.3.

ANUAR DE JESUS FERNANDEZ OLVERA received the B.Sc. degree in electronic and computer engineering from the Monterrey Institute of Technology and Higher Education (ITESM), Mexico, in 2010, the M.Sc. degree in electrical engineering from the Eindhoven University of Technology (TU/e), Eindhoven, The Netherlands, in 2015, and the Ph.D. degree from the Terahertz Devices and Systems Laboratory, Technical University of Darmstadt, Darmstadt, Germany. In 2016, he joined the Terahertz Devices and Systems Laboratory, Technical University of Darmstadt. His research interests include the development of terahertz systems, applications using photoconductive mixers, and theoretical modeling.

BENEDIKT LEANDER KRAUSE received the B.Sc. degree in electronic and sensor materials from the Technical University of Bergakademie Freiberg, Freiberg, Germany, in 2015, and the M.Sc. degree in electrical engineering from Friedrich-Alexander Universität Erlangen-Nürnberg, Erlangen, Germany, in 2019. He is currently pursuing the Ph.D. degree in electrical engineering with the Terahertz Devices and Systems Laboratory, Technical University of Darmstadt, Darmstadt, Germany. His current research involves the quasi-optical measurements of terahertz frequencies.

ANDRÉS BETANCUR-PÉREZ received the M.Sc. degree in telecommunications engineering from the Universidad de Antioquia, Medellin, Colombia, in 2014. He is currently pursuing the Ph.D. degree in electrical engineering with the Universidad Carlos III de Madrid, Madrid, Spain. He is currently an Associate Professor with the Electronics and Telecommunications Department, Instituto Tecnologico Metropolitano, Medellin, Colombia. His research involves photonic architectures for the generation and detection of high-quality terahertz signals for spectroscopy and communications.

UTTAM NANDI received the B.Tech. degree in electronics and communication engineering from the Indian Institute of Technology (IIT) Guwahati, Guwahati, India, in 2014, the M.Sc. degree in wireless, photonics and space engineering from the Chalmers University of Technology, Gothenburg, Sweden, in 2016, and the Ph.D. degree from the Technical University of Darmstadt, Darmstadt, Germany. In 2017, he joined the Terahertz Devices and Systems Laboratory, Technical University of Darmstadt. His research interests are focused on the development of terahertz pulsed receivers and emitters based on ErAs:In(Al)GaAs photoconductors.

CRISTINA DE DIOS received the Ph.D. degree in electrical engineering from the Universidad Carlos III de Madrid, Madrid, Spain, in 2010, for her work in ultrafast pulsed diode lasers and nonlinear pulse compression. She is currently an Associate Professor with the Department of Electronics Technology and a member of the Sensors and Instrumentation Techniques Group, Universidad Carlos III de Madrid. Her research interests include optical frequency comb generation techniques, nonlinear optical phenomena, sub-terahertz and millimeter wave photonic signal synthesis and detection, and photonic integrated technology oriented to the miniaturization of complex sensing architectures.

PABLO ACEDO (Member, IEEE) received the M.Sc. degree in telecommunication engineering from the Universidad Politecnica de Madrid, Madrid, Spain, in 1993, and the Ph.D. degree (Hons.) from the Universidad Carlos III de Madrid, Madrid, in 2000, for his work on heterodyne two color laser interferometry for fusion plasma diagnostics.

His doctoral work included the development of the first two color laser system based on Mid-IR sources for a Stellarator Fusion Device (Stellarator TJ-II, Laboratorio Nacional de Fusión, CIEMAT, Madrid) and the first two-color Nd:YAG system for a Fusion Device (Tokamak C-Mod Plasma Science and Fusion Centre, Massachusetts Institute of Technology), the later during several doctoral visits to MIT during the years 1996–1999. In 2002, he was appointed as an Assistant Professor by the Universidad Carlos III de Madrid, where he continued with the development of scientific instrumentation systems for fusion plasma diagnostics and biomedical applications. He has also directed nine research projects (European, national, and regional funding) and has participated in another 31 (five of them EU funded). Finally, it is worth mentioning his leadership in knowledge transfer activities, where he has been IP in 12 contracts with companies (INDRA, AIRBUS D&S, LWL, SEAC, among others) and participated in another six; works that have led to various patents. He was also the Promoter of the creation and development of the spin-off Luz WaveLabs. Nowadays, his interests continue to focus on the development of scientific instrumentation systems, sensors and circuits, and their application in fields, such as bioengineering and environmental measurements. He has authored or coauthored more than 130 articles in high-impact journals and communications to international congresses, including invited conferences and seminars. His research interests include the development of multimode laser sources (optical frequency combs) and their applications in photonic signal synthesis with the development of several architectures for the generation, detection, and processing of terahertz signals, leading several research projects, and contracts in this field.

SASCHA PREU (Member, IEEE) received the Diploma and Ph.D. degrees *(summa cum laude)* in physics from the Friedrich-Alexander Universität Erlangen-Nürnberg, Erlangen, Germany, in 2005 and 2009, respectively.

From 2004 to 2010, he was with the Max Planck Institute for the Science of Light, Erlangen. From 2010 to 2011, he was with the Department of Materials and Physics, University of California at Santa Barbara, CA, USA. From 2011 to 2014, he worked as the Chair of applied physics with Universität Erlangen-Nürnberg. He is currently a Full Professor with the Department of Electrical Engineering and Information Technology, Technical University of Darmstadt, Germany, leading the Terahertz Devices and Systems Laboratory. He has authored or coauthored more than 110 journal articles and published conference contributions. His research interests include the development of semiconductor-based terahertz sources and detectors, including photomixers, photoconductors and field effect transistor rectifiers, and terahertz systems constructed thereof. In 2017, he received the ERC Starting Grant for developing ultra-broadband, photonic terahertz signal analyzers. He also works on the applications of terahertz radiation, in particular the characterization of novel terahertz components and materials.